

The Visualization of Threats Using the Augmented Reality and a Remotely Controlled Robot*

Tomas Lazna*

* Central European Institute of Technology, Brno University of Technology, Brno, Czech Republic (e-mail: tomas.lazna@ceitec.vutbr.cz).

Abstract: This paper introduces multi-robotic system ATEROS which can be applied in the area of the chemical, biological, radiological and nuclear (CBRN) protection. Potential dangers are identified by robots working in the autonomous mode. One particular problem is addressed – how to present those dangers to a human operator of a robot working in the telepresence mode. The technique of the augmented reality is used as a solution. It is assumed that the autonomous robot provides georeferenced information about the danger. The remotely controlled robot Orpheus-X4 is equipped with a precise GNSS receiver working in Real Time Kinematic (RTK) mode which provides accurate self-localization and with a camera. Knowing both the position and the orientation of the camera as well as its parameters, it is possible to calculate position of the danger within a picture provided by the camera. The augmented reality was successfully implemented to the Orpheus-X4 for a zero tilt. It was applied in a scenario of the gamma radiation sources localization but can be expanded to other cases even outside the CBRN domain.

Keywords: augmented reality, mobile robot, GNSS, camera calibration, radiological sources

1. INTRODUCTION

Means of the modern warfare as well as the operation of modern industrial facilities suggest that chemical, biological, radiological and nuclear (CBRN) defense (ICRC (2014)) will have increasing importance. For example, some industrial facilities deal with dangerous chemical materials which may leak due to technological accidents. Sources of ionizing radiation can be found e.g. in hospitals; such sources might get lost or even deliberately stolen and dispersed in an urban zone by a 'dirty bomb'.

The dangers can be identified by the autonomous telepresence robotic system ATEROS developed at the Faculty of Electrical Engineering and Communication, Brno University of Technology (Kocmanova and Zalud (2015), Zalud et al. (2015)). It is a multi-robotic system for autonomous or supervised reconnaissance of dangerous or inaccessible areas, as well as the environment contamination measurement. ATEROS consists of a control station with one or more human operators and a group of heterogenous robots – small and big reconnaissance robot, a mapping robot, a drone, etc. Advanced user interface with virtual reality and telepresence was developed to make the control immersive and intuitive.

Once the points of interest are localized, they can be presented to a human operating robots via the telepresence using a technique called *augmented reality*. It can be defined as follows (Reality Technologies (2016)): *An enhanced version of reality where live direct or indirect views of physical real-world environments are augmented with superimposed computer-generated images over a user's view of the real-world, thus enhancing ones current perception of reality.* The idea is to calculate the position of points of interest within the image frame acquired by the on-board camera and then visualize them for the operator and optionally add detailed information on the point, such as the intensity and the spectrum of a radiological source. More detailed description of the augmented reality as well as its applications may be found in the scientific literature, e.g. (Huy et al. (2017), Maly et al. (2016)).

The paper is organized as follows. Section 2 provides description of the used robot and necessary equipment. Transformation required for calculating coordinates of a point within the coordinate system of the camera are presented in Section 3. The process of the camera calibration and calculation of the point's pixel position are described in Section 4. The results are presented in Section 5.

2. SYSTEM DESCRIPTION

The Orpheus-X4 is a mid-size four-wheeled reconnaissance robot with a differential drive it is part of the ATEROS system. The robot is equipped with sensor head with three degrees of freedom that carries cameras and a rangefinder. Its basic parameters can be found in Table 1 and are

* This work was supported by the European Regional Development Fund under the project Robotics for Industry 4.0 (reg. no. CZ.02.1.01/0.0/0.0/15_003/0000470). The completion of this paper was made possible by the grant No. FEKT-S-17-4234 - 'Industry 4.0 in automation and cybernetics' financially supported by the Internal science fund of Brno University of Technology.



Fig. 1. The photo of the Orpheus-X4

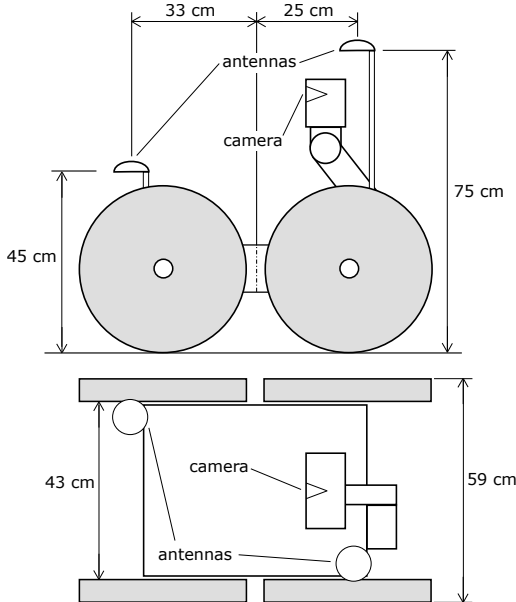


Fig. 2. The schematic picture of the Orpheus-X4

described in detail e.g. in Burian et al. (2014b). A photo of the Orpheus-X4 is provided in Fig. 1, its schematic picture featuring the key equipment can be found in Fig. 2.

Table 1. The parameters of the Orpheus-X4

Parameter	Value
Dimensions	950 × 590 × 415 mm
Weight	51 kg
Operation time	120 min
Drive type	Differential
Maximal speed	15 km·h ⁻¹

Beside the robotic platform, the system consists of a precise Global Navigation Satellite System (GNSS) receiver Trimble BD982 with the dual antenna input. The device works in the Real Time Kinematic (RTK) mode and therefore needs to receive correction data from the operator station equipped with another GNSS receiver. The system can measure the robot's position with the error under one centimeter. The self-localization and the navigation of the

robot are described in detail in Jilek (2015a) and Jilek (2015b).

The utilization of two rover antennas enables measurement of the robot's orientation; however, only partial information is provided. Beside the azimuth of the robot, the tilt is known; but its decomposition to roll and pitch components is not possible. Moreover, non-zero tilt induces error in the azimuth (yaw) measurement. Therefore, approximately zero tilt is considered in this paper for simplification. In order to measure all components of the orientation, it would be necessary to extend the system with an inertial measurement unit (IMU).

The robotic system includes miniature network camera AXIS P1214-E which is designed for outdoor surveillance (Axis Communications (2014)). It comprises a main unit which is hidden inside the robot and a separate sensor unit mounted in the robots sensor head. The sensor unit is equipped with 1/4" CMOS, it has both fixed iris (aperture F2.0) and fixed focus (2.8 mm). The field of view is equal to 81° horizontally and 44° vertically. It provides multiple H.264 streams with a resolution up to 720p. The device is powered over Ethernet which provides also the communication.

The robot is designed to be controlled via a technique called *visual telepresence*. Telemetric data are transferred to the operator station where they are visualized in the head mounted display (HMD) carried by the operator. Orientation of the HMD is measured using an IMU, transformed and sent back to the robot; its camera is then rotated accordingly. Consequently, the operator is able to look around in the place where the robot is and does not need to focus on the control of the camera; resulting system is more immersive and intuitive than a plain remote control. More information on the telepresence can be found in Zalud et al. (2014).

3. TRANSFORMATION OF COORDINATES

It is assumed that any danger can be represented by one or more points, e. g. vertices of a polygon. Coordinates of those points are known as well as instantaneous position of the robot in a common coordinate system; for example in WGS-84 (directly provided by the GNSS receiver). First, it is necessary to transform measured coordinates to a local Cartesian system. The chosen system has the *x*-axis parallel to circles of latitude (east is the positive direction), the *y*-axis is parallel to meridians (north is the positive direction). Points in WGS-84 have coordinates (ϕ, λ, h) where ϕ is the latitude, λ is the longitude and h is the height. In the local system, the point's position is described by (x, y, z) . Coordinates are transformed using rhumb lines (Movable Type (2017)). Rhumb line is a path of constant bearing which crosses all meridians at the same angle and is a straight line in the Mercator projection. Coordinates of a base station in WGS-84 are (ϕ_0, λ_0, h_0) and $(0, 0, h_0)$ in the local system; note that the *z*-coordinate is selected to be equal to the height in the WGS-84. The point to be transformed has coordinates (ϕ_1, λ_1, h_1) in WGS-84 and (x_1, y_1, h_1) in the local system. The point's *x*-coordinate is a rhumb-line distance between the base station and the point at the same latitude.

$$x_1 = \cos \phi_0 \cdot (\lambda_1 - \lambda_0) \cdot R \quad (1)$$

where R is the Earth's radius and is equal to 6,371,008 m (William (2016)). Similarly the y -coordinate is a rhumb-line distance between the base station and the point at the same longitude.

$$y_1 = (\phi_1 - \phi_0) \cdot R \quad (2)$$

Next, it is needed to transform coordinates of the point of interest to the coordinate system of the robot's camera. This transformation can be divided into series of elementary steps. Used coordinate system is denoted as follows:

- O_0 for the local Cartesian system to which are WGS-84 coordinates transformed,
- O_R for a system originating in the center of the robot,
- O_1, O_2, O_3 for systems originating in the first, second and third joint of the sensor head,
- O_C for a system originating in the optical center of the camera.

The transformation from system O_0 to system O_R can be generalized and used for any kind of robot, other transformations are platform-dependent. In the beginning, both coordinates of the point of interest (x_p, y_p, z_p) and of the center of the robot (x_0, y_0, z_0) are known in O_0 . Although the GNSS receiver measures coordinates of the main antenna, the self-localization module provides coordinates of the center as it is an important piece of information for the navigation. As it was mentioned earlier, zero tilt of the robot is assumed; therefore, systems O_0 and O_R have the same direction of the z -axis. The first transformation can be described by following equation using homogeneous transformation matrices (a detailed overview can be found, e.g., in Spong et al. (2005)).

$$\begin{pmatrix} x_R \\ y_R \\ z_R \\ 1 \end{pmatrix} = \begin{pmatrix} \cos \alpha & -\sin \alpha & 0 & 0 \\ \sin \alpha & \cos \alpha & 0 & 0 \\ 0 & 0 & 1 & 0 \\ 0 & 0 & 0 & 1 \end{pmatrix} \begin{pmatrix} 1 & 0 & 0 & -x_0 \\ 0 & 1 & 0 & -y_0 \\ 0 & 0 & 1 & -z_0 \\ 0 & 0 & 0 & 1 \end{pmatrix} \begin{pmatrix} x_p \\ y_p \\ z_p \\ 1 \end{pmatrix}, \quad (3)$$

where α is equal to the robot's azimuth -90° . The right angle is subtracted in order to rotate the coordinate system in a way that the x -axis of O_R heads in a forward direction of the robot (convention).

Next step is to transform coordinates to system O_3 ; thereby, all rotations of the sensor head are handled. A kinematic scheme of the head is shown in Fig. 3. The transformation is again described by homogeneous matrices in a following manner.

$$\begin{pmatrix} x_3 \\ y_3 \\ z_3 \\ 1 \end{pmatrix} = \begin{pmatrix} \cos q_3 & 0 & \sin q_3 & l_2 \\ 0 & 1 & 0 & 0 \\ -\sin q_3 & 0 & \cos q_3 & 0 \\ 0 & 0 & 0 & 1 \end{pmatrix} \begin{pmatrix} 1 & 0 & 0 & l_1 \\ 0 & \cos q_2 & -\sin q_2 & 0 \\ 0 & \sin q_2 & \cos q_2 & 0 \\ 0 & 0 & 0 & 1 \end{pmatrix} \begin{pmatrix} 1 & 0 & 0 & -x_{J1} \\ 0 & 1 & 0 & -y_{J1} \\ 0 & 0 & 1 & -z_{J1} \\ 0 & 0 & 0 & 1 \end{pmatrix} \begin{pmatrix} x_R \\ y_R \\ z_R \\ 1 \end{pmatrix}, \quad (4)$$

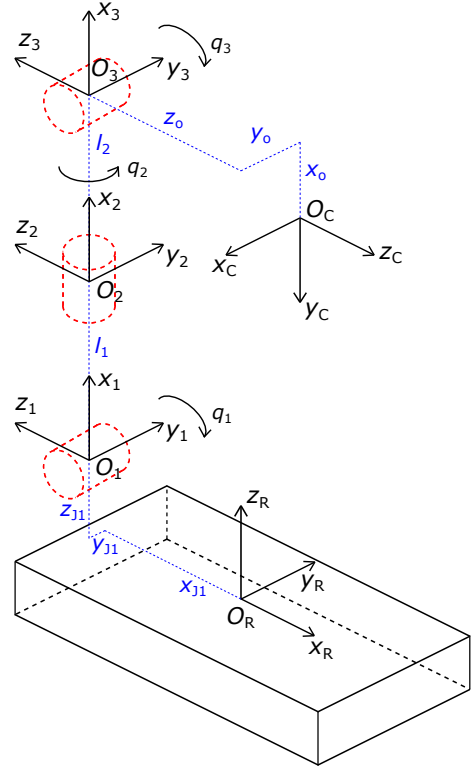


Fig. 3. The kinematic scheme of the sensor head

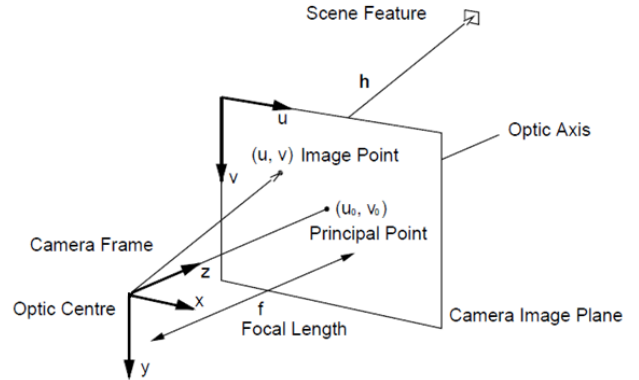


Fig. 4. The model of the camera (Davison (2002))

where q_1, q_2 and q_3 are rotational coordinates of the joints, x_{J1}, y_{J1} and z_{J1} are coordinates of the first joint in O_R and l_1, l_2 are negative distances between joints.

Finally, the coordinates need to be transformed to system O_C . This last transformation consists of translation to the optical center of the camera (its coordinates are (x_o, y_o, z_o) in O_3) and a transposition of axes in order to achieve the orientation shown in Fig. 4 which is conventional for cameras. The transformation is described by the equation:

$$\begin{pmatrix} x_C \\ y_C \\ z_C \\ 1 \end{pmatrix} = \begin{pmatrix} 0 & -1 & 0 & 0 \\ -1 & 0 & 0 & 0 \\ 0 & 0 & -1 & 0 \\ 0 & 0 & 0 & 1 \end{pmatrix} \begin{pmatrix} 1 & 0 & 0 & -x_o \\ 0 & 1 & 0 & -y_o \\ 0 & 0 & 1 & -z_o \\ 0 & 0 & 0 & 1 \end{pmatrix} \begin{pmatrix} x_3 \\ y_3 \\ z_3 \\ 1 \end{pmatrix}. \quad (5)$$

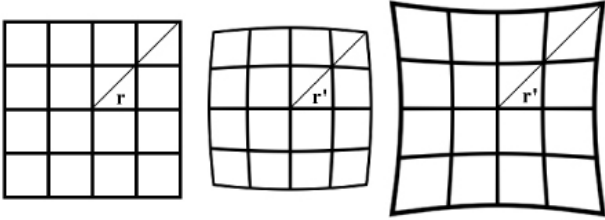


Fig. 5. The distortion of a rectangular grid; an undistorted grid on the left, a grid with the barrel distortion in the middle and a grid with the pincushion distortion on the right (Choi et al. (2006))

4. CAMERA CALIBRATION

According to Zhang (1999), a projection of a 3D point to a 2D point in an image plane of a camera is computed using transformation matrices shown below. The 3D point is denoted by $\mathbf{M} = (x, y, z)$, the 2D point is denoted by $\mathbf{m} = (u, v)$. It is beneficiary to use homogeneous coordinates, thus, the vectors \mathbf{M} and \mathbf{m} are augmented to $\tilde{\mathbf{M}}$ and $\tilde{\mathbf{m}}$ by adding 1 as the last element. The relationship between those vectors then follows the equation:

$$\tilde{\mathbf{m}} = \mathbf{A}(\mathbf{R}, \mathbf{t})\tilde{\mathbf{M}}, \quad (6)$$

where s is an arbitrary scale factor, (\mathbf{R}, \mathbf{t}) are extrinsic parameters of the camera and \mathbf{A} represents intrinsic parameters of the camera. The extrinsic parameters comprise rotation and translation of the camera in a world coordinate system in which the point coordinates \mathbf{M} are given. However, the arbitrary position and orientation of the camera were dealt with in the previous section; thus, the extrinsic parameters can be expressed as:

$$(\mathbf{R}, \mathbf{t}) = \begin{pmatrix} 1 & 0 & 0 & 0 \\ 0 & 1 & 0 & 0 \\ 0 & 0 & 1 & 0 \end{pmatrix}. \quad (7)$$

The intrinsic parameters are described by the matrix A :

$$\mathbf{A} = \begin{pmatrix} f_x & c & u_0 \\ 0 & f_y & v_0 \\ 0 & 0 & 1 \end{pmatrix}, \quad (8)$$

where (f_x, f_y) are focal lengths in the horizontal and the vertical axis, (u_0, v_0) are coordinates of the center of projection, or principal point, c describes the skewness of the image axes. So far, a lens distortion has not been taken into account. There are two types of distortion – a radial and a tangential. The latter can be neglected for common cameras such as the one used in the described robotic system. Effects of the radial distortion are shown in Fig. 5. The distortion is characterized by a pair of parameters k_1 , k_2 . In order to correct the distortion, coordinates in the image plane have to be updated according to the following equations (assuming $c = 0$):

$$\hat{u} = u + (u - u_0)[k_1(x^2 + y^2) + k_2(x^2 + y^2)^2] \quad (9)$$

$$\hat{v} = v + (v - v_0)[k_1(x^2 + y^2) + k_2(x^2 + y^2)^2] \quad (10)$$

To perform the projection properly, both intrinsic parameters and distortion coefficients of the camera need to be

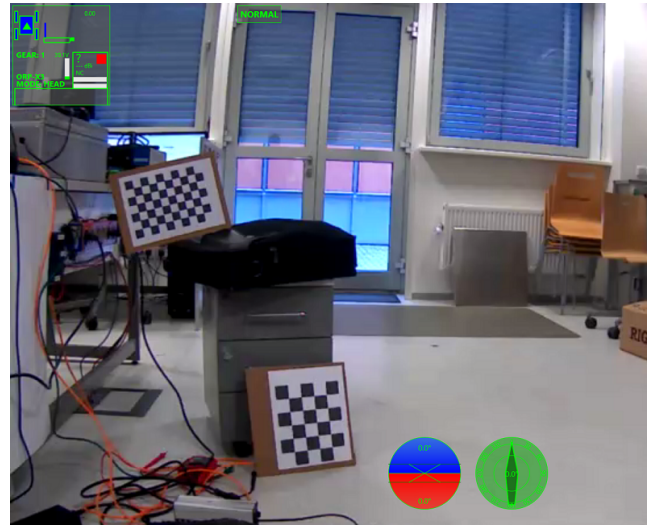


Fig. 6. An example of a calibration picture

identified. The process of identification is called *camera calibration*. It is based on taking several pictures of a calibration chessboard-like pattern with a different position and orientation. There are some tools that enable automated identification of the parameters. For the purposes of this paper, the GML C++ Camera Calibration Toolbox (Vezhnevets et al. (2013)), which uses the OpenCV library, has been utilized. An example of the calibration picture can be found in Fig. 6. It is recommended to take 8 images with two different calibration patterns present in the same time.

5. RESULTS

The presented projection of a point of interest was integrated to the Cassandra (Burian et al. (2014a)) – it is a system for the teleoperation of robots included in the multi-robotic system ATEROS. It provides the head-up display (HUD), alternatively status bar, which presents relevant information to the operator; e.g. the name of the controlled robot, the status of its actuators and the quality of the link.

To demonstrate capabilities of the presented system, radiological threats were chosen. The methodology for autonomous robotic localization of radiological sources can be found in Lazna et al. (2018). Another way to locate points of interest is e.g. utilizing a flight photogrammetry (Gabrlik et al. (2018)).

The Cassandra was provided with a list of radiological sources relevant for the current mission, i.e. sources found by other types of robots in the area of interest. The radiological source located in the field of view of the controlled robot's camera is represented by the ionizing radiation hazard trefoil. As the projection reduces one dimension, the symbol is appended with a distance of the robot from the source; the Euclidean distance is utilized. Finally, extra information about the source is included to the HUD; namely, the intensity of the source characterized by the dose rate in 1 meter and the spectrum of the source which can be used for estimating the type of the source (isotope).



Fig. 7. The experimental result

The system was verified with experiments in real conditions. The area of interest was chosen with regard to the desired zero tilt of the robot. The Orpheus-X4 was manually driven through the area while capturing the operator's screen. The result is shown in Fig. 7. Note that two prominent peaks are present near the center of the spectrum; an experienced operator can assume that the displayed source is Cobalt-60 which is characterized by those energies.

Two deficiencies of the described system were discovered during the experiment. First, the displayed symbol does not hold stable position in the screen. Second, there is delay between the rotation of the sensor head and the shift of the displayed symbol.

6. CONCLUSION

The robotic system Orpheus-X4 equipped with precise RTK GNSS receiver proved to be applicable in the field of outdoor augmented reality. Crucial parameters of the robot necessary for the implementation were identified as well as optical parameters of the used camera. Kinematic model of the robot's sensor head was described within this paper as well as corresponding transformations of coordinates.

The system was tested in real conditions; the test provided two subjects of possible improvement which were mentioned in the previous section. The chattering of the symbol on the screen is caused by the measurements inaccuracy. The self-localization is burdened with a noise which shown itself to be significant for distances of the robot and the object in the order of tens of meters. Theoretically, it is possible to filter data from the GNSS receiver but that would probably cause unwanted delay between fast change

of the robots position (e.g. rotation in spot) and corresponding alteration of the objects projection. The other improvement relating to a rotation of the sensor head is probably easy to manage; altering the type of information provided by the robot on the state of its actuators should be sufficient.

In the future, it is planned to integrate an IMU into the self-localization module. First, it enables measurement of remaining coordinates of the robot (two angles of the orientation roll and pitch). Consideration of the arbitrary rotation of the robot would make the system more general. Then, using fusion of data from multiple sources a reduction of the self-localization noise could be achieved (Schall et al. (2009)).

Presently, applicability of the proposed system is limited, however, it can be enhanced by suggested improvements. In the field of Industry 4.0, the utilization of robotic systems has increasing importance. A collaboration between human workers and robots is often addressed; the augmented reality represents a way of the human-machine interaction which is native for those workers.

REFERENCES

- Axis Communications. AXIS P1214-E network camera: Datasheet, 2014. URL https://www.axis.com/files/datasheet/ds_p1214e_1496754_en_1709.pdf. Accessed: 2018-03-06.
- Frantisek Burian, Petra Kocmanova, and Ludek Zalud. Robot mapping with range camera, CCD cameras and thermal imagers. In *2014 19th International Conference on Methods and Models in Automation and Robotics (MMAR)*, pages 200–205, September 2014a. doi: 10.1109/MMAR.2014.6957351.

- Frantisek Burian, Ludek Zalud, Petra Kocmanova, Tomas Jilek, and Lukas Kopecny. Multi-robot system for disaster area exploration. *WIT Transactions on Ecology and the Environment*, 184:263–274, June 2014b. doi: 10.2495/FRIAR140221.
- Kai San Choi, Edmund Y. Lam, and Kenneth K. Y. Wong. Automatic source camera identification using the intrinsic lens radial distortion. *Optics Express*, 14(24):11551–11565, November 2006. ISSN 1094-4087. doi: 10.1364/OE.14.011551.
- Andrew J. Davison. SLAM with a Single Camera. In *SLAM/CML Workshop at ICRA*, 2002.
- Petr Gabrlik, Anders la Cour-Harbo, Petra Kalvodova, Ludek Zalud, and Premysl Janata. Calibration and accuracy assessment in a direct georeferencing system for UAS photogrammetry. *International Journal of Remote Sensing*, 0(0):1–29, February 2018. ISSN 0143-1161. doi: 10.1080/01431161.2018.1434331.
- Dinh Quang Huy, I. Vietcheslav, and Gerald Seet Gim Lee. See-through and spatial augmented reality - a novel framework for human-robot interaction. In *2017 3rd International Conference on Control, Automation and Robotics (ICCAR)*, pages 719–726, April 2017. doi: 10.1109/ICCAR.2017.7942791.
- ICRC. *Chemical, Biological, Radiological and Nuclear Response: Introductory Guidance*. International Committee of the Red Cross, Geneva, Switzerland, March 2014.
- Tomas Jilek. Autonomous field measurement in outdoor areas using a mobile robot with RTK GNSS. *IFAC-PapersOnLine*, 28(4):480–485, 2015a. doi: 10.1016/j.ifacol.2015.07.081.
- Tomas Jilek. Radiation intensity mapping in outdoor environments using a mobile robot with RTK GNSS. 2015b. doi: 10.1109/MILTECHS.2015.7153755.
- Petra Kocmanova and Ludek Zalud. Multispectral Stereoscopic Robotic Head Calibration and Evaluation. In *Modelling and Simulation for Autonomous Systems*, Lecture Notes in Computer Science, pages 173–184. Springer, Cham, April 2015. ISBN 978-3-319-22382-7 978-3-319-22383-4. doi: 10.1007/978-3-319-22383-4\13.
- Tomas Lazna, Petr Gabrlik, Tomas Jilek, and Ludek Zalud. Cooperation between an unmanned aerial vehicle and an unmanned ground vehicle in highly accurate localization of gamma radiation hotspots. *International Journal of Advanced Robotic Systems*, 15(1), January 2018. ISSN 1729-8814. doi: 10.1177/1729881417750787.
- Ivo Maly, David Sedlacek, and Paulo Leitao. Augmented reality experiments with industrial robot in industry 4.0 environment. In *2016 IEEE 14th International Conference on Industrial Informatics (INDIN)*, pages 176–181, July 2016. doi: 10.1109/INDIN.2016.7819154.
- Movable Type. *Calculate distance and bearing between two Latitude/Longitude points using haversine formula in JavaScript*. Cambridge, 2017.
- Reality Technologies. What is Augmented Reality (AR)? Ultimate Guide to Augmented Reality (AR) Technology, 2016. URL <http://www.realitytechnologies.com/augmented-reality>. Accessed: 2018-03-06.
- Gerhard Schall, Dagner Wagner, Gerhard Reitmayer, Elise Taichmann, Manfred Wieser, Dieter Schmalstieg, and Bernhard Hofmann-Wellenhof. Global pose estimation using multi-sensor fusion for outdoor Augmented Reality. In *2009 8th IEEE International Symposium on Mixed and Augmented Reality*, pages 153–162, October 2009. doi: 10.1109/ISMAR.2009.5336489.
- Mark W. Spong, Seth Hutchinson, and M. Vidyasagar. *Robot Modeling and Control*. Wiley, November 2005. ISBN 978-0-471-64990-8.
- Vladimir Vezhnevets, Alexander Velizhev, Anton Yakubenko, and Nikita Chetverikov. GML C++ Camera Calibration Toolbox, Graphics and Media Lab, 2013. URL <http://graphics.cs.msu.ru/en/node/909>. Accessed: 2018-03-06.
- David R. William. *Earth Fact Sheet*. NASA Space Science Data Coordinated Archive, 2016.
- Ludek Zalud, Petra Kocmanova, Frantisek Burian, and Tomas Jilek. Color and Thermal Image Fusion for Augmented Reality in Rescue Robotics. In H. a. M. Sakim and M. T. Mustaffa, editors, *8th International Conference on Robotic, Vision, Signal Processing & Power Applications: Innovation Excellence Towards Humanistic Technology*, volume 291, pages 47–55. Springer, New York, 2014. ISBN 978-981-4585-42-2 978-981-4585-41-5. WOS:000337307100006.
- Ludek Zalud, Petra Kocmanova, Frantisek Burian, Tomas Jilek, Petr Kalvoda, and Lukas Kopecny. Calibration and Evaluation of Parameters in a 3D Proximity Rotating Scanner. *Elektronika Ir Elektrotehnika*, 21(1):3–12, 2015. ISSN 1392-1215. doi: 10.5755/j01.eee.21.1.7299. WOS:000349838500001.
- Zhengyou Zhang. Flexible camera calibration by viewing a plane from unknown orientations. In *Proceedings of the Seventh IEEE International Conference on Computer Vision*, volume 1, pages 666–673 vol.1, 1999. doi: 10.1109/ICCV.1999.791289.